Carbohydrate Polymers 101 (2014) 692–698

Contents lists available at ScienceDirect

Carbohydrate Polymers

journal homepage: www.elsevier.com/locate/carbpol

Acid pH-activated glycol chitosan/fullerene nanogels for efficient tumor therapy

Sol Kim[a,1], Dong Jin Lee[a,1], Dong Sup Kwag[a], Ung Yeol Lee[a], Yu Seok Youn[b], Eun Seong Lee[a,*]

[a] Division of Biotechnology, The Catholic University of Korea, 43-1 Yeokgok 2-dong, Wonmi-gu, Bucheon-si, Gyeonggi-do 420-743, Republic of Korea
[b] College of Pharmacy, Sungkyunkwan University, 300 Chonchon-dong, Jangan-gu, Suwon-si, Gyeonggi-do 440-746, Republic of Korea

ARTICLE INFO

Article history:
Received 16 August 2013
Received in revised form
27 September 2013
Accepted 30 September 2013
Available online 9 October 2013

Keywords:
Glycol chitosan
Fullerene conjugates
2,3-Dimethylmaleic acid
Photodynamic therapy

ABSTRACT

Glycol chitosan (GC) grafted with 2,3-dimethylmaleic acid (DMA) and fullerene (C_{60}) conjugates (GC-*g*-DMA-*g*-C_{60}) were developed for use in a photosensitizer prodrug. GC-*g*-DMA-*g*-C_{60} was prepared *via* the simple two-step chemical grafting reactions of (i) DMA to free amine groups of GC and (ii) hydroxyl groups of GC-*g*-DMA to π—π carbon bonds of C_{60}. This conjugate was self-assembled to form polysaccharidic nanogels consisting of a hydrophilic block (GC and DMA) and a hydrophobic block (C_{60}). Here, GC-*g*-DMA-*g*-C_{60} nanogels also formed multi-nanogel aggregates due to the electrostatic interaction between the pendant carboxylic acid group (due to the DMA) and residual free amine group of GC at pH 7.4. Interestingly, the nanogel aggregates can be disintegrated at pH 5.0 due to the reduction of electrostatic interaction resulting from the cleavage of the DMA blocks at pH 5.0. Upon 670 nm light illumination, photo-responsive properties of the nanogel aggregates allowed different singlet oxygen generation according to the pH condition: the reduced singlet oxygen generation (due to increased photo-interference effect between C_{60} molecules close-packed in nanogel aggregates) at pH 7.4, but the elevated singlet oxygen generation (due to the disintegration of nanogel aggregates) at pH 5.0. GC-*g*-DMA-*g*-C_{60} nanogel aggregates responds to pH 5.0 (∼endosomal pH) can be a good candidate for endosomal pH targeting and *in vivo* photodynamic therapy in various malignant tumor cells.

1. Introduction

The therapeutic benefit of photodynamic therapy (PDT) has gained considerable attention in antitumor applications because PDT utilizes external light illumination at the tumor sites for the generation of highly reactive oxygen species (such as singlet oxygen) from photosensitizer drugs systemically delivered to tumors (Bosi, Da Ros, Spalluto, & Prato, 2003; Chen, Ma, Liu, & Chen, 2012; Diener, Alford, Kennel, & Mirazdeh, 2007; Zhu et al., 2008). This method of tumor therapy provides promising modality for the treatment of local tumors illuminated by external light source, associated with ameliorated drug side effects for normal tissues (Bosi et al., 2003; Chen et al., 2012; Diener et al., 2007). However, most photosensitizer drugs used in PDT have been outside this expectation and exhibit limited clinical availability due to the lack of multifunctionality for improving drug therapeutic effects (Chen et al., 2012; Nakamura & Isobe, 2003; Tabata & Ikada, 1999; Wei, Zhang, Lu, Man, & Wen, 2010). Introduction of a novel photosensitizer drug tailor-made for this purpose can provide a means to overcome the aforementioned issue.

One of important trials in photosensitizer drug design is directed toward the incorporation of stimuli-responsive polymers (Lee, Oh, Baik, Youn, & Lee, 2010; Lee et al., 2011; Oh et al., 2010, 2012) to photosensitizer drugs. For example, our group recently reported a photosensitizer drug with an intelligent phototoxicity switch which was pH dependant (Park et al., 2011, 2012). This photosensitizer drug consists of glycol chitosan grafted with a functional 3-diethylaminopropyl isothiocyanate (DEAP), chlorin e6 (photosensitizer drug), and poly(ethylene glycol), which allowed relatively higher phototoxicity at tumor extracellular pH (∼pH 6.8), while minimizing phototoxicity at physiological pH (∼pH 7.4) (Park et al., 2011). These pH-dependent properties emphasize the potential of photosensitizer drugs for improved tumor therpay.

Fullerene (C_{60}), one of the photosensitizer chemicals, can readily transfers the exited energy to oxygen molecules during the light illumination at 670 nm, resulting in the generation of singlet oxygen in a high yield (Bosi et al., 2003; Chen et al., 2012; Diener et al., 2007). Several investigations for photosensitizer drug design have been made by utilizing exohedral derivatization methods using synthetic polymers, peptide/proteins, and antibodies (Bosi et al.,

* Corresponding author. Tel.: +82 2 2164 4921; fax: +82 2 2164 4865.
E-mail address: eslee@catholic.ac.kr (E.S. Lee).
[1] These authors equally contributed to this work.

0144-8617/$ – see front matter © 2013 Elsevier Ltd. All rights reserved.
http://dx.doi.org/10.1016/j.carbpol.2013.09.108

Table 1
Characterization of GC-*g*-DMA-*g*-C_{60}.

Sample	Conjugated DMA molecules per one repeating unit of GC[a]	Conjugated C_{60} molecules per one repeating unit of GC[b]
GCDF	0.57	0.11
GCF	0	0.09

[a, b] The conjugation of C_{60} (or DMA) to GC was estimated from ^{1}H NMR (DMSO-*d6* with TMS).

2003; Chen et al., 2012; Diener et al., 2007; Wen et al., 2012). However, even in the case of several exohedral fullerenes, there has been a lack of progress in pharmaceutical approaches due to poor functionalities in tumor therapy.

Here, we describe the facile synthesis of fullerene derivatives based on functionalized glycol chitosan (GC) for PDT. Glycol chitosan (GC) grafted with 2,3-dimethylmaleic acid (DMA) and fullerene (C_{60}) (GC-*g*-DMA-*g*-C_{60}) were synthesized *via* a simple two-step chemical grafting reaction of (i) DMA to free amine groups of GC and (ii) free hydroxyl groups of GC-*g*-DMA to π—π carbon bonds of C_{60} (Fig. 1a). It is interesting to note that the GC-*g*-DMA-*g*-C_{60} self-assembled in aqueous solution can form multi-nanogel aggregates due to the electrostatic interaction between pendant DMA groups and the residual free amine group of GC at pH 7.4. These nanogel aggregates can be divided into single nanogel parts at pH 5.0 due to the reduction of electrostatic interactions resulting from cleavage of the DMA blocks (Lee et al., 2010) at pH 5.0 (Fig. 1b). These changes in physicochemical properties will support the potential of GC-*g*-DMA-*g*-C_{60} nanogel aggregates for targeting endosomal pH (~pH 5.0) (Canton & Battaglia, 2012) in tumor cells. In this study, we preferentially investigated the pH-responsive properties of these nanogel aggregates, their singlet oxygen generation, and their phototoxicity toward malignant tumor cells.

2. Experimental

2.1. Materials

Fullerene (C_{60}) was purchased from NanoLab Inc. (Waltham, MA, USA). Glycol chitosan (GC, *Mw* = 500 kDa), 2,3-dimethylmaleic anhydride (DMA), dimethylsulfoxide (DMSO), triethylamine (TEA), 9,10-dimethylanthracene, lithium hydroxide (LiOH), pyridine, sodium borate ($Na_2B_4O_7$), and toluene were purchased from Sigma–Aldrich (St. Louis, MO, USA). RPMI-1640, fetal bovine serum (FBS), penicillin, and streptomycin were purchased from Welgene, Inc (Seoul, South Korea). The Cell Counting Kit-8 was obtained from Dojindo Molecular Technologies Inc (Kumamoto, Japan).

2.2. GC-g-DMA-g-C_{60} synthesis

GC (300 mg) was reacted with DMA (564 mg) in DMSO (20 mL) containing TEA (1.2 mL) and pyridine (1.2 mL) at room temperature for 3 days, yielding GC grafted with 2,3-dimethylmaleic acid (GC-*g*-DMA) (yield ~89%). GC-*g*-DMA or GC (200 mg) was coupled with C_{60} (143 mg) in toluene (50 mL)/DMSO (20 mL) co-solvent containing LiOH (23 mg) at room temperature for 7 days (Fig. 1a), yielding GC-*g*-DMA-*g*-C_{60} (GCDF) or GC-*g*-C_{60} (GCF) (Table 1). After the reaction, toluene was removed using a rotary evaporator, and the resulting solution was transferred to a pre-swollen dialysis membrane tube (Spectra/Por® MWCO 15K, Spectrum Lab. Inc., Rancho Dominguez, USA) and was dialyzed against sodium borate buffer (pH 7.4) solution to remove non-reacted chemicals. The solution withdrawn from a dialysis membrane tube was freeze-dried for 2 days (Kwag et al., 2012; Kwag, Park, Oh, & Lee, 2013). The yield of final products (GCDF or GCF) was ~84%.

2.3. Nanogel synthesis

GCDF or GCF (10 mg) were dissolved in DMSO (2 mL) and transferred to a pre-swollen dialysis membrane tube (Spectra/Por MWCO 15K), after which the solutions were dialyzed against 150 mM phosphate buffer saline (PBS, pH 7.4) for 24 h. The outer phase was replaced three times with fresh PBS solution (Kwag et al., 2012, 2013). The solution was subsequently freeze-dried for 2 days. The yield of nanogel synthesis was ~92%.

2.4. Particle size distribution

The particle size distribution of GCDF or GCF nanogels (1 mg/mL) at different pH values (pH 7.4–5.0, PBS 150 mM) was measured using a Zetasizer 3000 instrument (Malvern Instruments, Westborough, MA, USA) equipped with a He—Ne Laser beam at a wavelength of 632.8 nm and a fixed scattering angle of 90° (Kwag et al., 2012, 2013). Before the test, GCDF or GCF nanogels at different pHs (pH 7.4–5.0, PBS 150 mM) were stabilized at room temperature for 4 h. The morphology of GCDF or GCF nanogels was confirmed using a field emission scanning electron microscopy (FE-SEM, Hitachi s-4800, Tokyo, Japan).

2.5. Light transmittance

The light transmittance of solutions was measured using a UV–visible spectrophotometer (Labantech Co., USA) (Kwag et al., 2012, 2013). Before the test, GCDF or GCF nanogel solutions (1 mg/mL) at different pH (pH 7.4–5.0, PBS 150 mM) were stabilized at room temperature for 4 h. Relative transmittance of the GCDF or GCF nanogel solution was measured in the selected pH range with respect to transmittance at pH 7.4.

2.6. Zeta potential

The zeta potential of each sample (1 mg/mL) stabilized at different pH values (PBS 150 mM, pH 7.4–5.0) for 4 h was measured using a Zetasizer 3000 instrument (Malvern Instruments)

2.7. Singlet oxygen generation

The generation of singlet oxygen from GCDF or GCF nanogels was confirmed using 9,10-dimethylanthracene. First, GCDF, GCF nanogels (equivalent to 1 mg/mL C_{60}) or free C_{60} (1 mg/mL) at different pHs (pH 7.4–5.0, PBS 150 mM) were stabilized at room temperature for 4 h. The samples (equivalent to 1 mg/mL C_{60}) were mixed with 9,10-dimethylanthracene (20 mmol) in PBS (150 mM, pH 7.4) and were then illuminated at a light intensity of 100 mW/cm^2 using a 670 nm laser source for 10 min. Fluorescent 9,10-dimethylanthracene reacts selectively with singlet oxygen, resulting in decreased fluorescent intensity (Gomes, Fernandes, & Lima, 2005). The change of 9,10-dimethylanthracene fluorescence intensity in each sample was measured using a Shimadzu RF-5301PC spectrofluorometer at λ_{ex} 360 nm and λ_{em} 380–550 nm. When the fluorescence intensity of 9,10-dimethylanthracene reached a plateau after 1 h, the change in fluorescence intensity of 9,10-dimethylanthracene ($F_f - F_s$) was plotted after subtracting the fluorescence intensity of each sample (F_s) from the fluorescence intensity of full 9,10-dimethylanthracene (without the nanogels, indicating no singlet oxygen, F_f). All data were obtained by using the slit-width of excitation and the emission of the spectrofluorometer at 5 nm (Kwag et al., 2012, 2013).

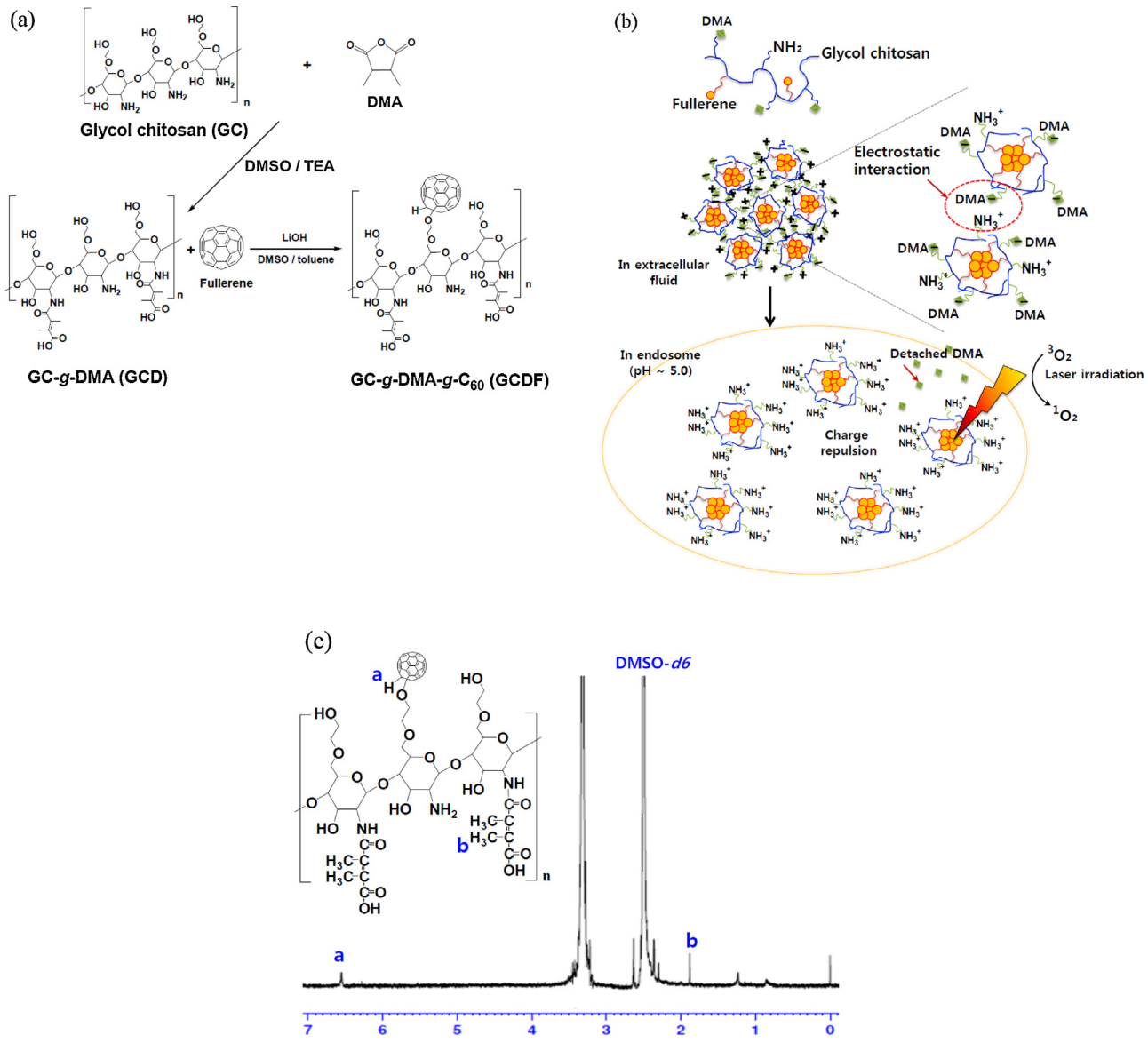

Fig. 1. (a) Synthesis scheme and (b) concept of purposed GC-*g*-DMA-*g*-C_{60} conjugates. (c) ^{1}H-NMR peak of GC-*g*-DMA-*g*-C_{60} conjugates.

2.8. *In vitro* phototoxicity

Human nasopharyngeal epidermal carcinoma KB cells were maintained in RPMI-1640 medium with 2 mM L-glutamine, 1% penicillin–streptomycin, and 10% FBS in a humidified standard incubator with a 5% CO_2 atmosphere at 37 °C. Prior to testing, cells (1×10^5 cells/mL) were grown as a monolayer, and were harvested *via* trypsinization using a 0.25% (w/v) trypsin/0.03% (w/v) EDTA solution. KB cells were suspended in RPMI-1640 medium and were seeded onto well plates and cultured for 24 h prior to *in vitro* cell testing (Kwag et al., 2012, 2013). Phototoxicity of GCDF or GCF nanogels with light illumination was tested in KB tumor cells. GCDF, GCF nanogels (equivalent to 0.1–10 mg/mL C_{60}) or free C_{60} (0.1–10 mg/mL C_{60}) dispersed in RPMI-1640 medium was administered to the cells. The cells were incubated with each sample for 12 h and were then washed three times with PBS (pH 7.4). The cells in in fresh RPMI-1640 medium were illuminated at a light intensity of 100 mW/cm^2, using a 670 nm laser source for 5 min and were then further incubated for 12 h without light illumination. Cell viability was determined using a Cell Counting Kit-8 (CCK-8 assay) (Lee, Ahn, Youn, & Lee, 2013).

In addition, to estimate the original toxicity of each sample, cell viability tests of KB cells treated with GCDF, GCF nanogels (equivalent to 1–50 mg/mL C_{60}) or free C_{60} (1–50 mg/mL C_{60}) for 24 h without light illumination was conducted.

2.9. *pH-activatable phototoxicity*

KB cells treated with GCDF or GCF nanogels (equivalent to 10 mg/mL C_{60}) were dispersed in RPMI-1640 medium (pH 7.4 or 5.0, adjusted using 0.1 M HCl or 0.1 M NaOH) for 30 min, and then illuminated at a light intensity of 10 mW/cm^2, using a 670 nm laser source for 5 min and then washed with fresh 150 mM PBS (pH 7.4). The cells in fresh RPMI-1640 medium were further incubated in fresh RPMI-1640 medium for 12 h. Cell viability was determined using CCK-8 assay in KB cells.

2.10. *Transmission electron microscopy (TEM) analysis*

The KB tumor cells, incubated with GCDF or GCF nanogels (equivalent to 10 mg/mL C_{60}) for 6 h at 37 °C, were washed three

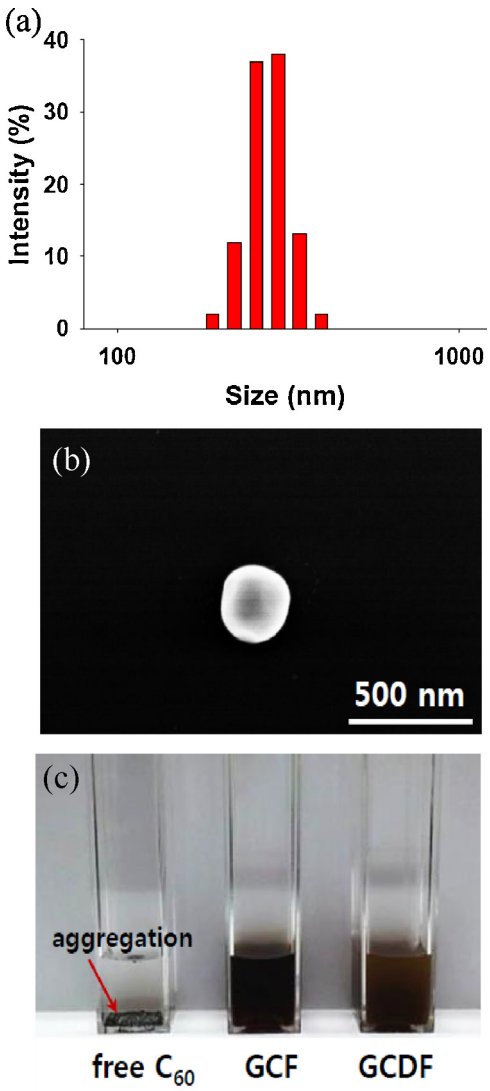

Fig. 2. (a) Particle size distribution and (b) FE-SEM image of GCDF nanogels (150 mM, pH 7.4, 1 mg/mL). (c) Optical image of free C_{60}, GCF or GCDF nanogels dispersed in PBS solution (150 mM, pH 7.4, 2 mg/mL).

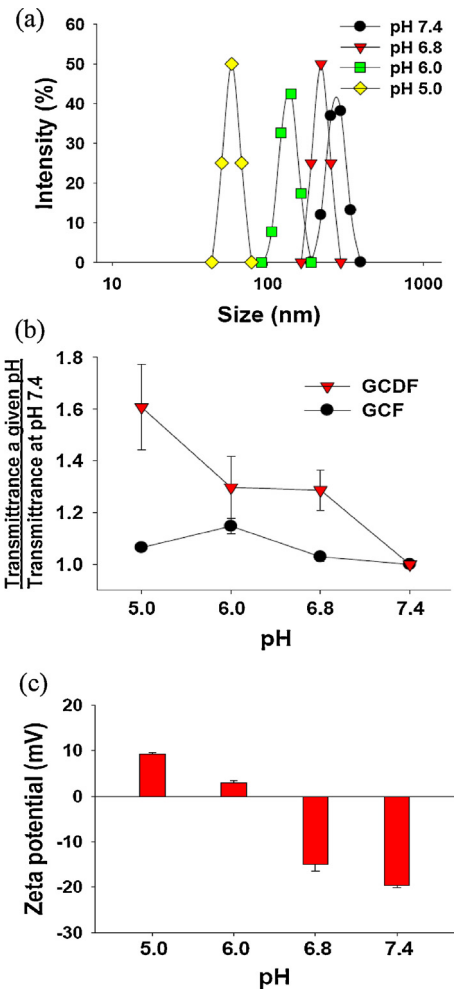

Fig. 3. Particle size change of GCDF nanogels (1 mg/mL) exposed at different pH values ($n = 3$). (b) The relative change of GCDF or GCF nanogels (1 mg/mL) in transmittance according to the pH of each solution ($n = 3$). (c) Zeta potential change of GCDF nanogels (1 mg/mL) exposed at different pH values ($n = 3$).

times with fresh PBS, and were then fixed in 4% paraformaldehyde/2.5% glutaraldehyde in 0.1 M PBS overnight. After washing with 0.1 M PBS, the specimens were post-fixed with 1% osmium tetroxide in PBS for 1 h. The specimens were then dehydrated with pure ethanol and embedded in Epon 812. The polymerization of Epon 812 was performed at 60 °C for 3 days. Ultra-thin sections (60–70 nm) from embedded specimens were obtained using an ultra-microtome (Leica Ultracut UCT, Germany). Ultra-thin sections were mounted onto carbon-coated copper grids and examined using TEM (JEM 1010, Japan) operating at 60 kV and CCD camera (SC1000 Orion, USA) (Kwag et al., 2013).

2.11. *In vivo* fluorescence imaging

In vivo studies were conducted with 4–6-week old female nude mice (BALB/c, nu/nu mice, Institute of Medical Science, Tokyo, Japan). Nude mice were maintained under the guidelines of an approved protocol from the Institutional Animal Care and Use Committee (IACUC) of the Catholic University of Korea (Republic of Korea).

For the *in vivo* animal experiments, KB tumor cells were introduced into female nude mice *via* subcutaneous injection of 1×10^5 cells suspended in PBS pH 7.4 (ion strength: 0.15) medium. When the tumor volume reached about 70 mm^3, the nanogels (equivalent to C_{60} 10 mg/kg mice body) were injected intravenously into tumor-bearing nude mice through the tail vein. A 12-bit CCD camera (Image Station 4000 MM; Kodak, Rochester, NY, USA) equipped with a special C-mount lens and a long wave emission filter (600–700 nm; Omega Optical, Brattleboro, VT, USA) was used to obtain live fluorescence images of the nude mice (Oh et al., 2012; Park et al., 2011). In addition, fluorescent images from wells containing GCDF nanogel solution (equivalent to 10–100 mg/mL C_{60}, PBS 150 mM, pH 7.4) were visualized with a KODAK image station ($\lambda_{excitation} = 635$ nm, $\lambda_{emission} = 720$ nm).

3. Results and discussion

3.1. Characterization of GC-*g*-DMA-*g*-C_{60}

GC-*g*-DMA was synthesized through the graft chemical reaction of DMA to free amine groups of GC. GC-*g*-DMA-*g*-C_{60} was then prepared through the coupling reaction between free hydroxyl groups of GC-*g*-DMA and π—π carbon bonds of C_{60} in the presence of LiOH (as a catalyst). The conjugation of DMA to GC was estimated from ^{1}H-NMR (DMSO-d_6 with TMS) from the peaks of δ 1.88 ppm (—CH_3 in DMA) and δ 3.30 ppm (—CH_2 in GC) (Fig. 1c). The conjugated DMA molecules for each repeating unit of GC was 0.57 (GCDF) (Table 1).

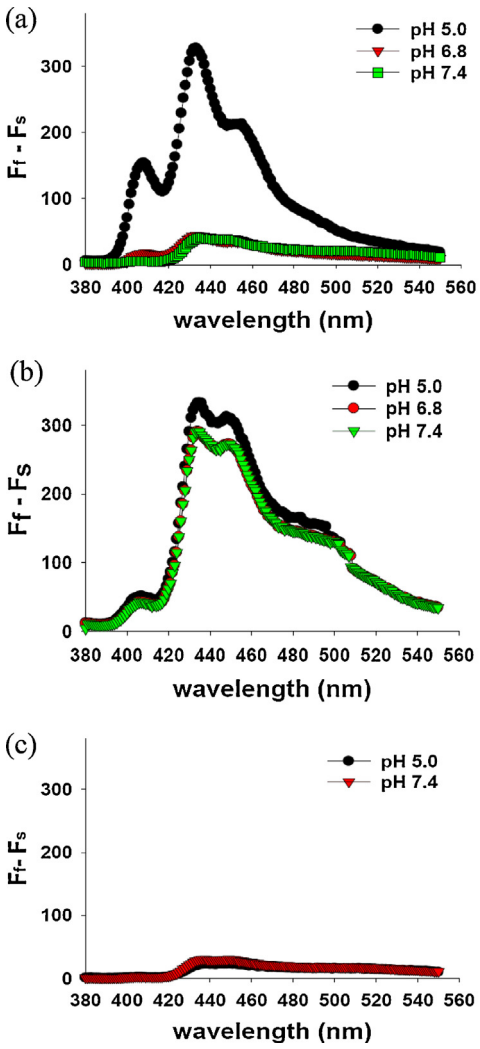

Fig. 4. The generation of singlet oxygen of (a) GCDF, (b) GCF nanogels (equivalent to 1 mg/mL C_{60}) or (c) free C_{60} (1 mg/mL) exposed at different pH values.

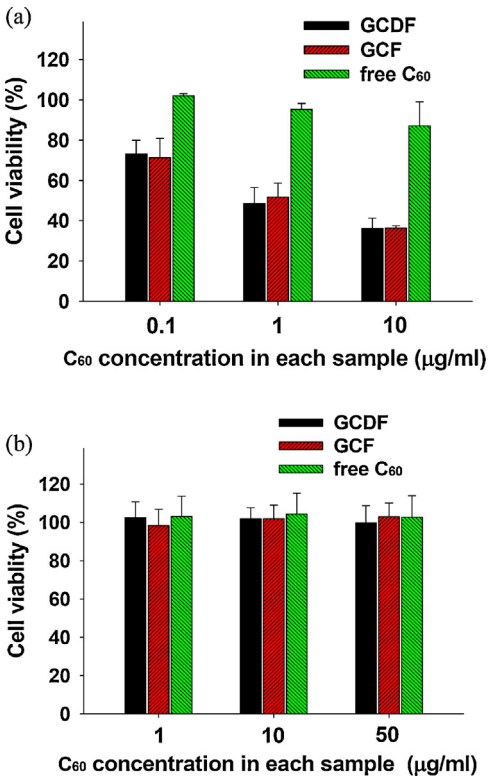

Fig. 5. (a) Phototoxicities were determined using a CCK-8 assay in KB cells treated with GCDF, GCF nanogels (equivalent to 0.1–10 mg/mL C_{60}) or free C_{60} (0.1–10 mg/mL) for 12 h with light illumination ($n = 7$). (b) Cell viabilities of KB cells treated with GCDF, GCF nanogels (equivalent to 1–50 mg/mL C_{60}) or free C_{60} (1–50 μg/mL) for 24 h without light illumination ($n = 7$).

The conjugation of C_{60} to GC was also estimated from ^{1}H-NMR (DMSO-d_6 with TMS) from the peaks of δ 6.55 ppm (—CH in C_{60}) and δ 3.30 ppm (—CH_2 in GC) (Fig. 1c). The conjugated C_{60} molecules per one repeating unit of GC were 0.11 (GCDF) or 0.09 (GCF) (Table 1).

3.2. *GC-g-DMA-g-C_{60} nanogel aggregates*

The GC-*g*-DMA-*g*-C_{60} nanogels were simply prepared by the self-assembling process (Hahn et al., 2007; Park et al., 2006) of GC and DMA blocks on a hydrophilic shell, and C_{60} blocks at the hydrophobic core using the dialysis method. Here, it is hypothesized that the GC-*g*-DMA-*g*-C_{60} nanogels can form multi-nanogel aggregates due to the electrostatic interactions of nanogels with the pendant carboxylic acid group (due to the DMA) and residual free amine group of GC. Fig. 2a shows that the average particle size of the GC-*g*-DMA-*g*-C_{60} (GCDF) nanogels was approximately 283 nm, which is comparable with the average particle size of the GC-*g*-C_{60} (GCF) nanogels without DMA blocks (approximately 46 nm) (data not shown). This difference in particle size indicates complicated nanostructure formation in GCDF. In addition, the image obtained from FE-SEM evidenced that GCDF nanogels are almost spherical (Fig. 2b), similar to those of GCF nanogels (data not shown). The GCDF or GCF nanogels exhibited effective dispersion in PBS (Fig. 2c). The GCDF or GCF nanogels were also stable for 2 week without any precipitation; the changes in the size of the nanogels were negligible (data not shown). However, as shown in Fig. 3a, the average particle size of GCDF nanogels changed from 283 nm (pH 7.4) to 221 nm (pH 6.8), 133 nm (pH 6.0), and 54 nm (pH 5.0), upon alteration of pH. While the particle size change of GCF nanogels was not significant upon pH reduction from 7.4 to 5.0 (data not shown). Fig. 3b shows the transmittance change of the nanogel solution according to changes in pH. As the pH of the solution declined from 7.4 to 5.0, the relative transmittance of the GCDF nanogel solution increased, which is consistent with the reduction of nanogel size in GCDF with decreasing pH (Fig. 3a). In addition, the GCF nanogels exhibited no significant difference in relative transmittance at the various tested pH values (Fig. 3b). Fig. 3c shows the change in zeta potential of the nanogels as a function of pH. The zeta potentials of GCDF nanogels changed from –19.5 mV to + 9 mV upon pH reduction from 7.4 to 5.0. However, the change in zeta potentials of GCF nanogels was negligble (data not shown). It is known that DMA-conjugated pirmary amine would occur as free primary amine at a slightly acidic pH due to the rapid hydrolysis of DMA (Lee et al., 2010; Oh et al., 2012). It seemed that the negative zeta potential, which originated from the DMA block, was offset by the cleavage of the DMA block (backing to cationic free amine groups in GC) at pH 5.0.

Overall, the changes in physicochemical properties of GCDF upon pH reduction from 7.4 to 5.0 indicate that the nanogel aggregates (283 nm size) were disintegrated to single nanogel parts (54 nm, similar to the particle size of GCF nanogels) at pH 5.0 due to the reduction of electrostatic interactions between the nanogels by the cleavage of the anionic DMA blocks (Fig. 1b). As a result, the conjugation of GC-*g*-DMA to C_{60} seemed to be greatly influence the physicochemical properties of C_{60}.

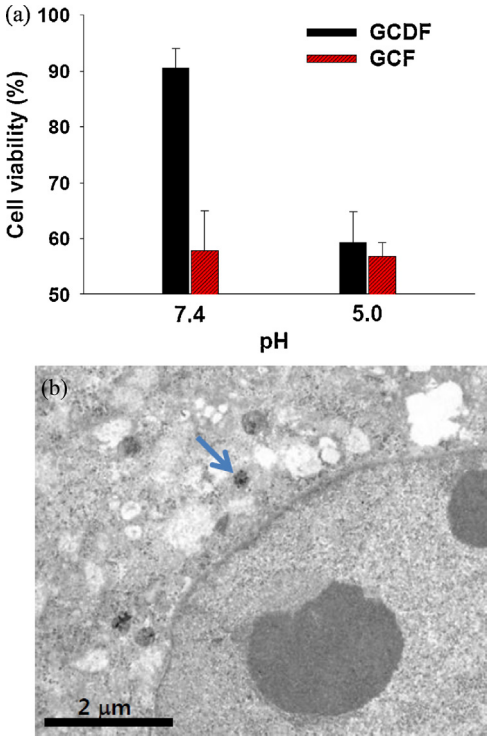

Fig. 6. (a) pH-activatable phototoxicity of GCDF or GCF nanogels (30 min treatment) at pH 7.4 or 5.0 with light illumination. ($n = 7$). (b) TEM analysis of KB tumor cells treated with GCDF nanogels (equivalent to 10 mg/mL C_{60}) for 6 h at 37 °C. The GCDF nanogels in the endosome are indicated by a blue arrow. (For interpretation of the references to color in this figure legend, the reader is referred to the web version of the article.)

3.3. Singlet oxygen generation from GC-g-DMA-g-C_{60} nanogels

Fig. 4 shows the singlet oxygen generation from GCDF, GCF or free C_{60} during light illumination (100 mW/cm^2 at 670 nm). The changes in fluorescence intensity ($F_f - F_s$) of 9,10-dimethylanthracene (dectector for singelet oxygen) (Gomes et al., 2005) reveal singlet oxygen generation from the nanogels or free C_{60}. The GCDF nanogels exhibited a reduced generation of singlet oxygen at pH 7.4–6.8, owing to the self-quenching event (due to increased photo-interference effect between C_{60} molecules close-packed in nanogel aggregates), which was recovered at pH 5.0 owing to the disintergration of nanogel aggregates. This is comparable with the pH-independent singlet oxygen generation of GCF nanogels (Fig. 4b) and the reduced singlet oxygen generation of free C_{60} molecules due to the poor solubility in water (Fig. 4c). These data support that GC-g-DMA-g-C_{60} nanogels can respond to pH 5.0 (similar to endosomal pH) and selectively generate singlet oxygen upon light illumination. These nanogels can be a good candidate for endosomal pH targeting and photodynamic antitumor therapy.

3.4. In vitro/in vivo evaluation

Fig. 5 shows the *in vitro* antitumor therapeutic efficiency of GCDF nanogels. The photodynamic cell ablation of GCDF, GCF or free C_{60} under light illumination was tested for human nasopharyngeal epidermal carcinoma KB cells. The GCDF, GCF nanogels (equivalent to 0.1–10 mg/mL C_{60}) or free C_{60} (0.1–10 mg/mL) dispersed in RPMI-1640 medium was administered to the cells. The cells were then incubated for 12 h. During these procedures, the nanogels undergo endocytosis and entrapment in acidic compartments (*e.g.*, endosomes) in KB tumor cells (Canton & Battaglia, 2012; Nam et al., 2009). Throughout this endocytic internalization pathway (Canton & Battaglia, 2012) the GCDF in the endosomes (~pH 5.0) are active for light illumination. As a result, GCDF and GCF nanogels led to relatively high levels of KB cell ablation upon light illumination at 670 nm (100 mW/cm^2) for 5 min. However, free C_{60} caused less phototoxicity of KB tumor cells. In addition, GCDF, GCF nanogels or free C_{60} prior to light illumination were not cytotoxic (Fig. 5b).

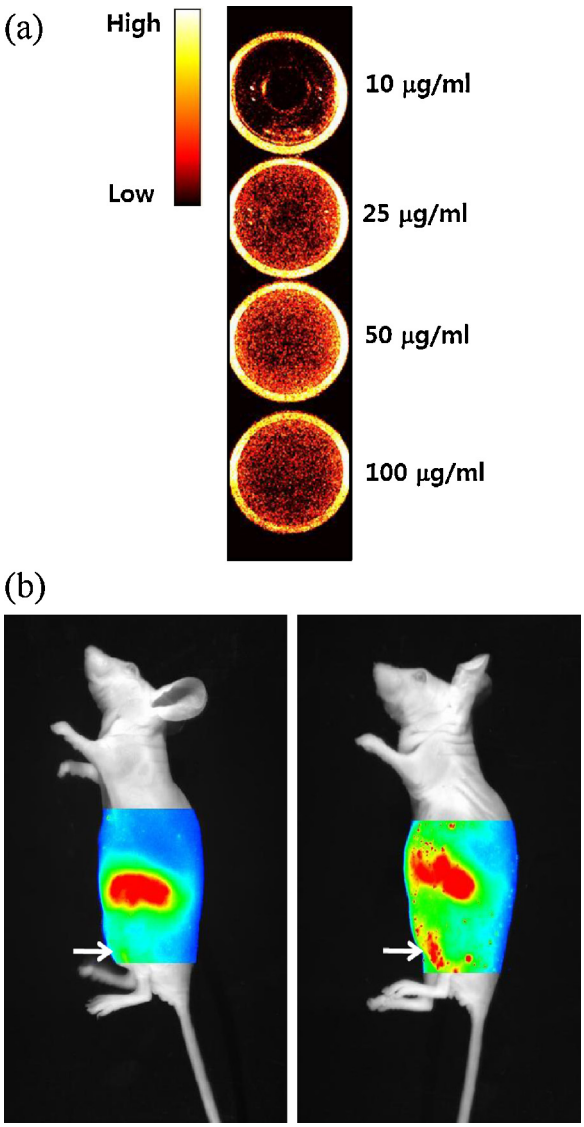

Fig. 7. (a) Near infra-red (NIR) fluorescence ($\lambda_{excitation} = 635$ nm, $\lambda_{emission} = 720$ nm) image from wells containing GCDF nanogels (equivalent to 10–100 mg/mL C_{60}) in 150 mM PBS (pH 7.4). (b) *In vivo* non-invasive fluorescent imaging of nude mice harboring KB tumors. A GCDF (equivalent to C_{60} 10 mg/kg mice body) was intravenously injected into nude mice and fluorescent images were obtained at 2 h (left) or 8 h (right) post-injection. Tumor site is indicated by a white arrow.

In an attempt to further evaluate the potential of GCDF as a photosensitizer for tumor therapy, KB tumor cells were incubated with GCDF or GCF nanogels (equivalent to 10 mg/mL C_{60}) at pH 7.4 or 5.0. A relatively short incubation period (30 min) limits the endocytosis of nanogels (Canton & Battaglia, 2012). We illuminated the cells at a light intensity of 10 mW/cm^2 using a 670 nm laser source for 5 min and determined the phototoxicities of the nanogels. It was found that the self-quenched GCDF at pH 7.4 allowed relatively lower phototoxicity for KB tumor cells, while the disintegrated GCDF at pH 5.0 displayed relatively increased KB cell ablation (Fig. 6a). These results are comparable with the high phototoxicities of GCF nanogels at all tested pH values. In addition,

the TEM images (Fig. 6b) reveal that endocytosed GCDF nanogels were efficiently disintegrated to single nanogel parts, suggesting the possibility of high phototoxicity in the endosomes upon light illumination.

Fig. 7 shows fluorescent images of the nanogels upon light illumination. It is known that hydroxyl group conjugation (breaking π—π carbon bonds of C_{60}) to C_{60} using LiOH as a catalyst influences the electronic emission state of C_{60}, resulting in a strong near-infrared (NIR) fluorescence intensity (Kwag et al., 2013). The C_{60} conjugates enable photo-luminescent tumor imaging without labeling any fluorophores or isotope. In Fig. 7a, fluorescent intensity of GCDF nanogels according to the C_{60} concentration was visualized with a KODAK image station ($\lambda_{excitation}$ = 635 nm, $\lambda_{emission}$ = 720 nm). Furthermore, we obtained *in vivo* fluorescent images of KB tumor-bearing nude mice after the intravenous injection of GCDF or GCF through the tail veins of nude mice (Fig. 7b). The GCDF nanogels allowed for high-resolution fluorescent intensity at the tumor site after 8 h, which may be due to the extravasation of nanogels from the tumor vasculature due to the enhanced permeability and retention (EPR) effect (Maeda & Matsumura, 2011). These results suggest that pH-responsive GC-*g*-DMA-*g*-C_{60} nanogels can be applied to *in vivo* photodynamic therapy and *in vivo* photo-luminescent imaging in various malignant tumor cells. Of course, to substantiate our findings of its potential, further investigations, such as *in vivo* animal test, will be required.

4. Conclusion

The GC-*g*-DMA-*g*-C_{60} nanogels exhibited an advanced property for endosomal pH targeting, through an enhanced singlet oxygen generation at pH 5.0, and elevated photodynamic tumor cell ablation at pH 5.0. The GC-*g*-DMA-*g*-C_{60} nanogels hold great promise for use in the selective endosomal delivery of photosensitizer drugs for tumors. We conclude that these qualities of GC-*g*-DMA-*g*-C_{60} nanogels are expected to improve the utility of C_{60} for photodynamic antitumor therapy.

Acknowledgements

This work was financially supported by a grant from the National R&D Program for Cancer Control, Ministry for Health and Welfare, Republic of Korea (No. 1320130), and by the GRRC program of Gyeonggi province [GRRC 2013-B01, Development of industrial nano-/micro-sized biomaterials for high performance drug release control].

References

Bosi, S., Da Ros, T., Spalluto, G., & Prato, M. (2003). Fullerene derivatives: An attractive tool for biological applications. *European Journal of Medicinal Chemistry*, *38*, 913–923.

Canton, I., & Battaglia, G. (2012). Endocytosis at the nanoscale. *Chemical Society Reviews*, *41*, 2718–2739.

Chen, Z., Ma, L., Liu, Y., & Chen, C. (2012). Applications of functionalized fullerenes in tumor theranostics. *Theranostics*, *2*, 238–250.

Diener, M. D., Alford, J. M., Kennel, S. J., & Mirazdeh, S. (2007). (212)Pb@C_{60} and its water-soluble derivatives: Synthesis, stability, and suitability for radioimmunotherapy. *Journal of the American Chemical Society*, *129*, 5131–5138.

Gomes, A., Fernandes, E., & Lima, J. L. (2005). Fluorescence probes used for detection of reactive oxygen species. *Journal of Biochemical and Biophysical Methods*, *65*, 45–80.

Hahn, U., Gegout, A., Duhayon, C., Coppel, Y., Saquet, A., & Nierengarten, J. F. (2007). Self-assembly of fullerene-rich nanostructures with a stannoxane core. *Chemical Communications*, *5*, 516–518.

Kwag, D. S., Oh, N. M., Oh, Y. T., Oh, K. T., Youn, Y. S., & Lee, E. S. (2012). Photodynamic therapy using glycol chitosan grafted fullerenes. *International Journal of Pharmaceutics*, *431*, 204–209.

Kwag, D. S., Park, K., Oh, K. T., & Lee, E. S. (2013). Hyaluronated fullerenes with photoluminescent and antitumoral activity. *Chemical Communications*, *49*, 282–284.

Lee, D. J., Ahn, Y. S., Youn, Y. S., & Lee, E. S. (2013). Poly(ethylene glycol)-crosslinked fullerenes for high efficient phototherapy. *Polymers for Advanced Technologies*, *24*, 220–227.

Lee, B. R., Oh, K. T., Baik, H. J., Youn, Y. S., & Lee, E. S. (2010). A charge-switched nano-sized polymeric carrier for protein delivery. *International Journal of Pharmaceutics*, *392*, 78–82.

Lee, B. R., Oh, K. T., Oh, Y. T., Baik, H. J., Park, S. Y., Youn, Y. S., et al. (2011). A novel pH-responsive polysaccharidic ionic complex for proapoptotic (KLAKLAK)2 peptide delivery. *Chemical Communications*, *47*, 3852–3854.

Maeda, H., & Matsumura, Y. (2011). EPR effect based drug design and clinical outlook for enhanced cancer chemotherapy. *Advanced Drug Delivery Reviews*, *63*, 129–130.

Nakamura, E., & Isobe, H. (2003). Functionalized fullerenes in water. The first 10 years of their chemistry, biology, and nanoscience. *Accounts of Chemical Research*, *36*, 807–815.

Nam, H. Y., Kwon, S. M., Chung, H., Lee, S. Y., Kwon, S. H., Jeon, H., et al. (2009). Cellular uptake mechanism and intracellular fate of hydrophobically modified glycol chitosan nanoparticles. *Journal of Controlled Release*, *135*, 259–267.

Oh, N. M., Kwag, D. S., Park, S. Y., Oh, K. T., Youn, Y. S., & Lee, E. S. (2012). Electrostatic charge conversion processes in engineered tumor-identifying polypeptides for targeted chemotherapy. *Biomaterial*, *33*, 1884–1893.

Oh, N. M., Oh, K. T., Baik, H. J., Lee, B. R., Lee, A. H., Youn, Y. S., et al. (2010). A self-organized 3-diethylaminopropyl-bearing glycol chitosan nanogel for tumor acidic pH targeting: Evaluation. *Colloids and surfaces B: Biointerfaces*, *78*, 120–126.

Park, S. Y., Baik, H. J., Oh, Y. T., Oh, K. T., Youn, Y. S., & Lee, E. S. (2011). A smart polysaccharide/drug conjugate for photodynamic therapy. *Angewandte Chemie International Edition*, *50*, 1644–1647.

Park, J. H., Kwon, S., Lee, M., Chung, H., Kim, J. H., Kim, Y. S., et al. (2006). Self-assembled nanoparticles based on glycol chitosan bearing hydrophobic moieties as carriers for doxorubicin: In vivo biodistribution and anti-tumor activity. *Biomaterials*, *27*, 119–126.

Park, S. Y., Oh, N. M., Oh, Y. T., Oh, K. T., Youn, Y. S., & Lee, E. S. (2012). Artificial photosensitizer drug network for mitochondria-selective photodynamic therapy. *Chemical Communications*, *48*, 2522–2524.

Tabata, Y., & Ikada, Y. (1999). Biological functions of fullerene. *Pure and Applied Chemistry*, *71*, 2047–2053.

Wei, P., Zhang, L., Lu, Y., Man, N., & Wen, L. (2010). C60(Nd) nanoparticles enhance chemotherapeutic susceptibility of cancer cells by modulation of autophagy. *Nanotechnology*, *21*, 495101.

Wen, A. M., Ryan, M. J., Yang, A. C., Breitenkamp, K., Pokorski, J. K., & Steinmetz, N. F. (2012). Photodynamic activity of viral nanoparticles conjugated with C60. *Chemical Communications*, *48*, 9044–9046.

Zhu, J., Ji, Z., Wang, J., Sun, R., Zhang, X., Gao, Y., et al. (2008). Tumor-inhibitory effect and immunomodulatory activity of fullerol $C_{60}(OH)_x$. *Small*, *4*, 1168–1175.